Cogn Neurodyn (2013) 7:505–521
DOI 10.1007/s11571-013-9254-0

RESEARCH ARTICLE

Stability switches and double Hopf bifurcation in a two-neural network system with multiple delays

Zi-Gen Song · Jian Xu

Received: 8 September 2012 / Revised: 22 March 2013 / Accepted: 8 April 2013 / Published online: 16 April 2013

Abstract Time delay is an inevitable factor in neural networks due to the finite propagation velocity and switching speed. Neural system may lose its stability even for very small delay. In this paper, a two-neural network system with the different types of delays involved in self- and neighbor-connection has been investigated. The local asymptotic stability of the equilibrium point is studied by analyzing the corresponding characteristic equation. It is found that the multiple delays can lead the system dynamic behavior to exhibit stability switches. The delay-dependent stability regions are illustrated in the delay-parameter plane, followed which the double Hopf bifurcation points can be obtained from the intersection points of the first and second Hopf bifurcation, i.e., the corresponding characteristic equation has two pairs of imaginary eigenvalues. Taking the delays as the bifurcation parameters, the classification and bifurcation sets are obtained in terms of the central manifold reduction and normal form method. The dynamical behavior of system may exhibit the quasi-periodic solutions due to the Neimark-Sacker bifurcation. Finally, numerical simulations are made to verify the theoretical results.

Keywords Neural network · Multiple delays · Stability switches · Double Hopf bifurcation · Quasi-periodic behavior

Z.-G. Song · J. Xu (✉)
School of Aerospace Engineering and Applied Mechanics, Tongji University, Shanghai 200092, China
e-mail: xujian@tongji.edu.cn

Z.-G. Song
College of Information Technology, Shanghai Ocean University, Shanghai 201306, China
e-mail: zigensong@163.com

Introduction

Time delay is an inevitable factor in the signal transmission between biological neurons or electronic-model-neurons due to the finite propagation velocity and switching speed (Campbell 2007; Sun et al. 2010). The neural network with time delays can be described by a class of infinite-dimensional delayed differential equations. To study the effect of time delay on neural systems, Marcus and Westervelt (1989) improved the Hopfield neural network by introducing delay-coupling into the nonlinear activation function. Due to the existence of time delay, some complex dynamic phenomena can be easily obtained near the equilibrium point of neural system.

It is well known that neural system may lose its stability by making the equilibrium point unstable even for very small delays. However, effect of time delay is an interesting problem. For example, in field of machine tool industry, the disturbance of the pure regeneration (one single delay) by e.g. variable angle distribution between milling edges, time variation of the delay can increase the stability of the cutting process (Budak 2003; Zatarain et al. 2008). A small delay is sufficient to destabilize a system, but a large delay may stabilize a system (Liao and Lu 2011; Ye and Cui 2012). This implies that time delays can induce system to exhibit the multi-stable regions, which is called the delay-dependent stability regions. The system behavior switches from being stable to unstable and then back to stable as delay increases. As early as 1980s, Cooke and Grossman (1982) constructed a delayed system with at least N times switching. Hale and Huang (1993) investigated a linear differential equation and obtained some global geometrical characteristics of the stability regions located in two-delayed plane. For the general linear delayed systems consisting of multiple delays, the stability

regions have been shown in two-delayed plane (Gu et al. 2005, 2007) and three-delayed space (Sipahi and Delice 2009; Gu and Naghnaeian 2011; Sipahi et al. 2011). Multiple delays can induce the stability switching of linear dynamical systems.

Bifurcation is one of the most important dynamical phenomena for the nonlinear neural systems (Jia et al. 2012; Liebovitch et al. 2011). Different bifurcations can lead to different kinds of dynamic behaviors. For example, Hopf bifurcation gives rise to the periodical activity, while double Hopf bifurcation results in two types of oscillations with different frequencies and a quasi-periodic behavior. Hopf bifurcation and periodical activity for neural network models with one single delay have been investigated extensively, see, e.g., Liao et al. (2007), Yuan and Li (2010), Guo and Huang (2003), Yan (2006) and the references cited therein. Due to the complexity of multiple delays, the analysis of stability and Hopf bifurcation for the multi-delayed differential equations is far from complete. Many researchers tried to fill in some "piece of the puzzle" for the multiple delays problem (Li et al. 1999). Considered the average/sum of time delays as the variable parameter and used the time-scale transformation, some multiple-delayed neural network systems with simple architecture can be transformed to the equivalent models with one single delay (Cao and Xiao 2007; Mao and Hu 2008; Wei and Zhang 2008).

In order to get a deep and clear understanding for multiple delays on dynamical behaviors, many researchers focused on the neural network systems with two delays, which are relatively simple. The stability and Hopf bifurcation for some special system with two delays have been investigated, such as neural system (Xu et al. 2006; Xu 2008), Lotka-Volterra predator–prey system (Nakaoka et al. 2006; Song et al. 2004), epidemic model (Cooke et al. 1996), tumor growth (Shi et al. 2011; Xu 2009), plastic deformation instability (Hilout et al. 2010), Mackey–Glass system (Li and Jiang 2011; Wan and Wei 2009), and so on. In 1994, Bélair and Campbell (1994) considered a simple motor control system with two negative delayed feedback loops. The stability regions of the equilibrium point are analyzed in the parameter (A, τ_2) plane for the fixed delay τ_1. In addition, the criticality of the Hopf bifurcation was considered in detail in terms of some numerical simulations. The result shows that the first order differential equation containing two delays can exhibit the double Hopf bifurcation. Similar analysis for the neural network with multiple delays can be referred in (Shayer and Campbell 2000; Yuan and Campbell 2004; Campbell et al. 2006). This approach can obtain a "piecewise global" perception for the bifurcation diagram in the multi-delayed system. However, to the best of our knowledge, in the existing relative literatures, there are few researchers chosen the multiple delays as the independent parameters for the dynamics analysis. The mutual effect of multiple delays on system dynamical behavior has been not considered yet. It is our research motivation in the present paper. In terms of the stability analysis of the corresponding linear part, the bifurcation points with high co-dimensional singularity and the bifurcation diagram are presented in the two-delayed plane for the neural network system.

To study the two-delayed effects on neural system in detail, in this paper, a codimension-two singularity, namely the double Hopf bifurcation, is analyzed employing the multiple delays as the bifurcation parameters. Various dynamical behaviors are classified in the neighborhood of the singularity point. The bifurcation sets consisting of the oscillation behaviors with the different frequencies and quasi-periodic state are obtained in the delay parameter plane in terms of the central manifold reduction and normal form method (Orosz and Stepan 2004; Dombovari et al. 2008), which was introduced firstly by Faria and Magalhaes (1995a, b). The double Hopf bifurcation analysis for the differential equation with one single delay can be found in some existing works, such as (Yu et al. 2002; Xu et al. 2007; Xu and Pei 2008). This approach provides a convenient tool to compute a relatively simple form of the original differential equation, which can be used to analyze the system dynamic behaviors.

Neural system considered in this paper is described by the following differential equation:

$$\begin{cases} \dfrac{dx(t)}{dt} = -x(t) + a_1 S(x(t-\tau_1)) + a_2 S(y(t-\tau_2)) + P, \\ \dfrac{dy(t)}{dt} = -y(t) + a_3 S(x(t-\tau_2)) + a_4 S(y(t-\tau_1)) + Q, \end{cases} \tag{1}$$

where $x(t)$ and $y(t)$ represent the neural behaviors at time t, a_1, a_2, a_3 and a_4 denote the coupled weights, τ_1 and τ_2 are the signal transmission delays for the self- and neighbor-connection, respectively, P and Q are the external inputs, the neuron activation function in $S(u)$ is given by $S(u) = 1/(1 + e^{-u})$.

For neural network (1), when the self-connection delay $\tau_1 = 0$, our previous works have illustrated that system exhibits the complex dynamical behaviors for the different values of time delay and external input (Song and Xu 2009). The types of equilibrium points are studied analytically in details in terms of the characteristic equation and static bifurcation. The central manifold reduction and normal form method are employed to determine the Hopf bifurcation and its stability. In addition, time delay can affect the existence of the Bogdanov-Takens bifurcation

(refer to Song and Xu 2012a). For some delayed interval, system may exhibit the saddle-node homoclinic bifurcation. Furthermore, when the variation slope ratio is proposed to the sigmoid activation function S, the dynamical behaviors of system (1) with $\tau_1 = \tau_2 = \tau$ may exhibit the chaotic behavior (Song and Xu 2012b).

The paper is organized as follows. Firstly, the local asymptotic stability of equilibrium point for system (1) is investigated by analyzing the corresponding characteristic equation of the linearized system. General stability criteria involving the time delays are obtained. The results show that stability switches may occur for some interval of delay τ_1 when τ_2 increases. In section "Existence of double Hopf bifurcation", the stability regions and Hopf bifurcation curves are illustrated in the delay (τ_1, τ_2) parameter plane. The double Hopf bifurcation points can be obtained from the intersection points of the first and second Hopf bifurcation, i.e., the characteristic equation has double imaginary eigenvalue with multiplicity two. In section "Central manifold reduction", regarding two delays as the bifurcation parameters, the typical dynamic behaviors near the double Hopf bifurcation are investigated in detail in terms of the central manifold reduction and normal form method. The system may exhibit the quasi-periodic solutions due to the Neimark-Sacker bifurcation. Finally, numerical simulations are made to verify the theoretical results. Conclusions are given in the last section.

Linear stability switches

The equilibrium point (x_0, y_0) for system (1) is the solution of the following equations:

$$\begin{cases} x_0 = a_1 S(x_0) + a_2 S(y_0) + P, \\ y_0 = a_3 S(x_0) + a_4 S(y_0) + Q. \end{cases} \tag{2}$$

To translate (x_0, y_0) to the trivial equilibrium point, letting $x \to x - x_0$ nd $y \to y - y_0$ one has the linearized equation of system (1) given by

$$\begin{cases} \dfrac{dx(t)}{dt} = -x(t) + a_1 \alpha x(t-\tau_1) + a_2 \beta y(t-\tau_2), \\ \dfrac{dy(t)}{dt} = -y(t) + a_3 \alpha x(t-\tau_2) + a_4 \beta y(t-\tau_1). \end{cases} \tag{3}$$

where $\alpha = S'(x_0)$, $\beta = S'(y_0)$. The corresponding characteristic equation of system (3) is

$$\begin{vmatrix} -1 - \lambda + a_1 \alpha e^{-\lambda \tau_1} & a_2 \beta e^{-\lambda \tau_2} \\ a_3 \alpha e^{-\lambda \tau_2} & -1 - \lambda + a_4 \beta e^{-\lambda \tau_1} \end{vmatrix} = 0, \tag{4}$$

namely

$$\begin{aligned} \Delta(\lambda, \tau_1, \tau_2) =& 1 - (a_1\alpha + a_4\beta)e^{-\lambda\tau_1} + a_1 a_4 \alpha\beta e^{-2\lambda\tau_1} \\ & - a_2 a_3 \alpha\beta e^{-2\lambda\tau_2} + (2 - (a_1\alpha + a_4\beta)e^{-\lambda\tau_1})\lambda \\ & + \lambda^2 = 0, \end{aligned} \tag{5}$$

It is well known that the equilibrium point is locally asymptotically stable if and only if each of eigenvalues has negative real parts. It follows that the boundary of the stability region can be determined by equations $\lambda = 0$ and $\lambda = i\omega$ ($\omega > 0$). However, from the dynamical bifurcation theory, the typical static bifurcation is exhibited as the parameters varying near $\lambda = 0$. That is to say, system exhibits the different number of equilibrium point when the eigenvalue passes through the imaginary axis along the real axis (Song and Xu 2012a, b). However, in this paper, we just investigate the stability switches induced by multiple delays. Since time delay can not change the number of the equilibrium point, in the following section, the purely imaginary eigenvalues $\lambda = i\omega$ ($\omega > 0$) for the characteristic equation (5) are only studied. For simplify, the investigation begins with the case $\tau_2 = 0$ in (5) as follows

$$\begin{aligned} \Delta(\lambda, \tau_1, 0) =& 1 - a_2 a_3 \alpha\beta - (a_1\alpha + a_4\beta)e^{-\lambda\tau_1} + a_1 a_4 \alpha\beta e^{-2\lambda\tau_1} \\ & + (2 - (a_1\alpha + a_4\beta)e^{-\lambda\tau_1})\lambda + \lambda^2 = 0. \end{aligned} \tag{6}$$

Without loss of generality, letting $\tau_1 = 0$ in (6) implies

$$\begin{aligned} \Delta(\lambda, 0, 0) =& 1 - a_1\alpha - a_4\beta + a_1 a_4 \alpha\beta - a_2 a_3 \alpha\beta \\ & + (2 - a_1\alpha - a_4\beta)\lambda + \lambda^2 = 0. \end{aligned} \tag{7}$$

It follows from the Routh-Hurwitz criterion that the necessary and sufficient conditions for all roots of (7) having negative real parts is given by

$$1 - a_1\alpha - a_4\beta + a_1 a_4 \alpha\beta - a_2 a_3 \alpha\beta > 0, \tag{8}$$

and

$$2 - a_1\alpha - a_4\beta > 0. \tag{9}$$

This implies that the equilibrium point (x_0, y_0) is locally asymptotically stable if the parameters are satisfied with the conditions of (8) and (9). With the time delay τ_1 varying, system (1) will lose the stability. To obtain such critical values of time delay, supposing $\lambda = iv$ ($v > 0$) is a pair of purely imaginary roots of (6), one has

$$\begin{aligned} \Delta(iv, \tau_1, 0) =& 1 - a_2 a_3 \alpha\beta - (a_1\alpha + a_4\beta)e^{-iv\tau_1} + a_1 a_4 \alpha\beta e^{-2iv\tau_1} \\ & + i(2 - (a_1\alpha + a_4\beta)e^{-iv\tau_1})v - v^2 = 0. \end{aligned} \tag{10}$$

Separating (10) into the real and imaginary parts yields

$$\begin{cases} (1 + a_1a_4\alpha\beta - a_2a_3\alpha\beta - v^2)\cos v\tau_1 - 2v\sin v\tau_1 \\ \qquad - (a_1\alpha + a_4\beta) = 0, \\ 2v\cos v\tau_1 + (1 - a_1a_4\alpha\beta - a_2a_3\alpha\beta - v^2)\sin v\tau_1 \\ \qquad - (a_1\alpha + a_4\beta)v = 0. \end{cases} \tag{11}$$

Taking the square, adding the equations and performing some simplification processes, we have

$$L(v) = v^8 + m_1v^6 - m_2v^4 + m_3v^2 + m_4 = 0, \tag{12}$$

where

$$\begin{aligned} m_1 &= 4 - (a_1^2\alpha^2 + a_4^2\beta^2 + 2a_1a_4\alpha\beta - 4a_2a_3\alpha\beta), \\ m_2 &= 6 + (2a_1^3a_4\alpha^3\beta + 2a_1a_4\alpha\beta(-3 - 2a_2a_3\alpha\beta + a_4^2\beta^2) \\ &\quad + a_1^2\alpha^2(-3 - 2a_2a_3\alpha\beta + 2a_4^2\beta^2) \\ &\quad - 3a_4^2\beta^2 + 2a_2a_3\alpha\beta(2 + 3a_2a_3\alpha\beta - a_4^2\beta^2)), \\ m_3 &= 4 - (3a_1^3\alpha^2 + 2\alpha(2a_2a_3 + a_1a_4(3 - 2a_1^2\alpha^2))\beta \\ &\quad + (3a_4^2 + 4(a_2a_3 - a_1a_4)(a_2a_3 + a_1a_4)\alpha^2 \\ &\quad + a_1^2(a_2a_3 - a_1a_4)^2\alpha^4)\beta^2 + 2\alpha(-2a_1a_4^3 \\ &\quad + (a_1a_2^2a_3^2a_4 + a_1^3a_4^3 - 2a_2^3a_3^3)\alpha^2)\beta^3 + a_4^2(a_2a_3 - a_1a_4)^2\alpha^2\beta^4), \\ m_4 &= ((a_2a_3 + a_1a_4)\alpha\beta - 1)^2(1 + a_1\alpha + \beta(a_4 - a_2a_3\alpha \\ &\quad + a_1a_4\alpha))(1 - \beta(a_4 + a_2a_3\alpha) + a_1\alpha(a_4\beta - 1)). \end{aligned}$$

Without loss of generality, letting (12) has a number of positive and simple roots $v_i = 1, 2, \ldots$, one has the following critical delays

$$\tau_{1,j}^i = (\varphi_i + 2j\pi)/v_i, \quad i = 1, 2, \cdots; \quad j = 0, 1, 2, \cdots, \tag{13}$$

where $\varphi_i \in [0, 2\pi)$ and satisfied with

$$\begin{cases} \cos(\varphi_i) = \dfrac{-(a_1\alpha + a_4\beta)(-1 + a_1a_4\alpha\beta + a_2a_3\alpha\beta - v_i^2)}{a_2^2a_3^2\alpha^2\beta^2 - a_1^2a_4^2\alpha^2\beta^2 - 2a_2a_3\alpha\beta(1 - v_i^2) + (1 + v_i^2)^2}, \\ \sin(\varphi_i) = \dfrac{-(a_1\alpha + a_4\beta)v_i(1 - a_1a_4\alpha\beta + a_2a_3\alpha\beta + v_i^2)}{a_2^2a_3^2\alpha^2\beta^2 - a_1^2a_4^2\alpha^2\beta^2 - 2a_2a_3\alpha\beta(1 - v_i^2) + (1 + v_i^2)^2}. \end{cases} \tag{14}$$

In order to determine whether the real part of eigenvalue increases or decreases when delay τ_1 crosses the critical values $\tau_{1,j}^i$, $\quad i = 1, 2, \cdots; j = 0, 1, 2, \cdots$.

Differentiating λ with respect to τ_1 in (10) reaches

$$\lambda'(\tau_1) = \frac{2a_1a_4\alpha\beta\lambda - e^{\lambda\tau_1}(a_1\alpha + a_4\beta)\lambda(1 + \lambda)}{2e^{2\lambda\tau_1}(1 + \lambda) - 2a_1a_4\alpha\beta\tau_1 + e^{\lambda\tau_1}(a_1\alpha + a_4\beta)(-1 + \tau_1 + \lambda\tau_1)}. \tag{15}$$

Moreover, as shown in Hu and Wang (2002), one obtains

$$\operatorname{sgn}\left\{\operatorname{Re}\left[\frac{d\lambda(\tau_1)}{d\tau_1}\bigg|_{\tau_1=\tau_{1,j}^i, \lambda=iv_i}\right]\right\} = \operatorname{sgn}\left[\frac{dL(v)}{dv}\bigg|_{v=v_i}\right]. \tag{16}$$

Therefore, based on the conditions of (8) and (9), one obtains the effect of delay τ_1 on the eigenvalue of characteristic equation (6) by using the transversality condition (16) and the Hopf bifurcation theorem of functional differential equation. When the polynomial $L(v)$ has no positive real root, all eigenvalues of the characteristic equation (6) have negative real parts for the arbitrary τ_1. If $L(v)$ has only one positive and simple root (not multiple root) v_0 satisfied with $dL(v)/dv|_{v=v_0} > 0$, there exists the critical delayed value $\tau_1^c > 0$ such that all the eigenvalues of the characteristic equation (6) have negative real parts for $\tau_1 \in (0, \tau_1^c)$ and at least one root has a positive real part for $\tau_1 > \tau_1^c$. Furthermore, if $L(v)$ has two positive and simple roots $0 < v_1 < v_2$ satisfied with $dL(v)/dv|_{v=v_1} > 0 (< 0)$ and $dL(v)/dv|_{v=v_2} < 0 (> 0)$, there exist a finite number of the delayed τ_1 intervals in which all eigenvalues of the characteristic equation (6) have negative real parts. However, when $L(v)$ has at least three positive and simple roots $0 < v_1 < v_2 < v_3 < \ldots$, the distribution of eigenvalues in the complex plane is very complexity.

In order to investigate the effect of multiple delays on the local stability of equilibrium point, we regard τ_2 as the varying parameter for any fixed delay τ_1. Letting $\lambda = i\omega$ ($\omega > 0$) is the simple root of characteristic equation (5), one obtains

$$\begin{aligned} \Delta(i\omega, \tau_1, \tau_2) &= 1 - (a_1\alpha + a_4\beta)e^{-i\omega\tau_1} + a_1a_4\alpha\beta e^{-2i\omega\tau_1} \\ &\quad - a_2a_3\alpha\beta e^{-2i\omega\tau_2} + i(2 - (a_1\alpha + a_4\beta)e^{-i\omega\tau_1}) \\ &\quad \times \omega - \omega^2 = 0. \end{aligned}$$

Separating the real and imaginary parts gives

$$\begin{cases} (1 - \omega^2 - (a_1\alpha + a_4\beta)\omega\sin(\omega\tau_1) - (a_1\alpha + a_4\beta)\cos(\omega\tau_1) \\ \qquad + a_1a_4\alpha\beta\cos(2\omega\tau_1) - a_2a_3\alpha\beta\cos(2\omega\tau_2) = 0, \\ 2\omega - (a_1\alpha + a_4\beta)\omega\cos(\omega\tau_1) + (a_1\alpha + a_4\beta)\sin(\omega\tau_1) \\ \qquad - a_1a_4\alpha\beta\sin(2\omega\tau_1) + a_2a_3\alpha\beta\sin(2\omega\tau_2) = 0. \end{cases} \tag{17}$$

Eliminating τ_2 from (17), one has

$$G(\omega,\tau_1)=\omega^4+n_1\omega^3+n_2\omega^2+n_3\omega+n_4=0, \tag{18}$$

where

$$\begin{aligned}
n_1 &= 2(a_1\alpha+a_4\beta)\sin(\omega\tau_1),\\
n_2 &= 2+(a_1\alpha+a_4\beta)^2-2(a_1\alpha+a_4\beta)\cos(\omega\tau_1)\\
&\quad -2a_1a_4\alpha\beta\cos(2\omega\tau_1),\\
n_3 &= 2[(a_1\alpha+a_4\beta)(1+a_1a_4\alpha\beta)-4a_1a_4\alpha\beta\cos(\omega\tau_1)]\\
&\quad \times\sin(\omega\tau_1),\\
n_4 &= 1+(a_1^2\alpha^2+a_4^2\beta^2+(a_1a_4\alpha\beta)^2+2a_1a_4\alpha\beta-(a_2a_3\alpha\beta)^2)\\
&\quad -2(a_1\alpha+a_4\beta)(1+a_1a_4\alpha\beta)\cos(\omega\tau_1)+2a_1a_4\alpha\beta\cos(2\omega\tau_1).
\end{aligned}$$

If (18) has a number of positive and simple roots ω_i, $i=1,2,\ldots$, then (5) has a series of critical delays

$$\tau_{2,j}^{i}=(\varphi_i+2j\pi)/\omega_i, i=1,2,\cdots;j=0,1,2,\cdots, \tag{19}$$

where $\varphi_i\in[0,2\pi)$ and satisfied with

$$\begin{cases}
\cos(2\varphi_i)=\dfrac{1-\omega_i^2-(a_1\alpha+a_4\beta)\omega_i\sin(\omega_i\tau_1)}{a_2a_3\alpha\beta}\\
\quad -\dfrac{(a_1\alpha+a_4\beta)\cos(\omega_i\tau_1)-a_1a_4\alpha\beta\cos(2\omega_i\tau_1)}{a_2a_3\alpha\beta},\\
\sin(2\varphi_i)=\dfrac{-2\omega_i+(a_1\alpha+a_4\beta)\omega_i\cos(\omega_i\tau_1)}{a_2a_3\alpha\beta}\\
\quad -\dfrac{(a_1\alpha+a_4\beta)\sin(\omega_i\tau_1)-a_1a_4\alpha\beta\sin(2\omega_i\tau_1)}{a_2a_3\alpha\beta}.
\end{cases} \tag{20}$$

To make sure the occurrence of the Hopf bifurcation, it is needed to check the transversality condition. Without loss of generality, the time delay τ_2 is chosen as the bifurcation parameter. The necessary condition for the existence of the Hopf bifurcation is that the critical eigenvalues cross the imaginary axis with non-zero velocity. Differentiating λ with respect to τ_2 in (5), one reaches

$$\frac{d\lambda}{d\tau_2}=\frac{-2a_2a_3\alpha\beta\lambda e^{2\lambda\tau_2}}{e^{\lambda(\tau_1+2\tau_2)}(2e^{\lambda\tau_1}(1+\lambda)+(a_1\alpha+a_4\beta)((1+\lambda)\tau_1-1))+2\alpha\beta(a_2a_3e^{2\lambda\tau_1}\tau_2-a_1a_4e^{2\lambda\tau_2}\tau_1)}. \tag{21}$$

It follows that

$$\operatorname{sgn}\left\{\operatorname{Re}\left[\frac{d\lambda(\tau_2)}{d\tau_2}\bigg|_{\tau_2=\tau_{2,j}^{i},\lambda=i\omega_i}\right]\right\}=\operatorname{sgn}\left[\frac{dG(\omega,\tau_1)}{d\omega}\bigg|_{\omega=\omega_i}\right]. \tag{22}$$

Based on the transversality condition (22) and the Hopf bifurcation theorem, one has the following assertions when each eigenvalue of the characteristic equation (6) has negative real part. If (18) has no positive root, the equilibrium point of system (1) is locally asymptotically stable for the arbitrary delay τ_2, which is called the delay-independent stability. On the other hand, if (18) has one simple positive root ω_0 satisfied with $dG(\omega,\tau_1)/d\omega|_{\omega=\omega_0}>0$, there exists only a critical delay value denoted by τ_c. All eigenvalues of system (1) have strictly negative real parts for $\tau_2\in[0,\tau_c)$, while at least one of eigenvalues with positive real part for $\tau_2\in[\tau_c,+\infty)$. The equilibrium point of system loses its stability via a Hopf bifurcation. The direction and stability of the Hopf bifurcation can be studied by means of the central manifold reduction and normal form method (Song and Xu 2012c). Furthermore, if $G(\omega,\tau_1)$ has two positive and simple roots $0<\omega_1<\omega_2$ satisfied with $dG(\omega,\tau_1)/d\omega|_{\omega=\omega_1}>0(<0)$ and $dG(\omega,\tau_1)/d\omega|_{\omega=\omega_2}<0(>0)$, there exist a finite number of the delayed τ_2 intervals in which all eigenvalues of the characteristic equation (5) have negative real parts. It implies that there exist a finite number of delayed intervals. If time delay is fixed into these intervals, the equilibrium point is locally asymptotically stable, while instable for the outside of the delayed ranges. That is to say, the system dynamic switches from stable to unstable, and then back to stable when delay increases and crosses the critical delayed values.

For example, we choose the coupled weights and external inputs as $a_1=-6$, $a_2=2.5$, $a_3=2.5$, $a_4=-6$, $P=0.4$ and $Q=0.4$, respectively. The time delays of self- and neighbor-connection, namely τ_1 and τ_2 are considered as the variable parameters. The figures of function G (18) and eigenvalue real parts of (5) are displayed in Fig. 1 for the different self-connection delay τ_1, where the eigenvalue real parts are obtained with the aid of the numerical tool DDE BIFTOOL (Engelborghs et al. 2002). Figure 1a shows that the curve determined by function G and the line $G=0$ have not intersection point when $\omega>0$ holds. It implies that function G (18) exhibits no positive real root for the fixed delay $\tau_1=1$. The real parts of all eigenvalues have the negative part, as shown in

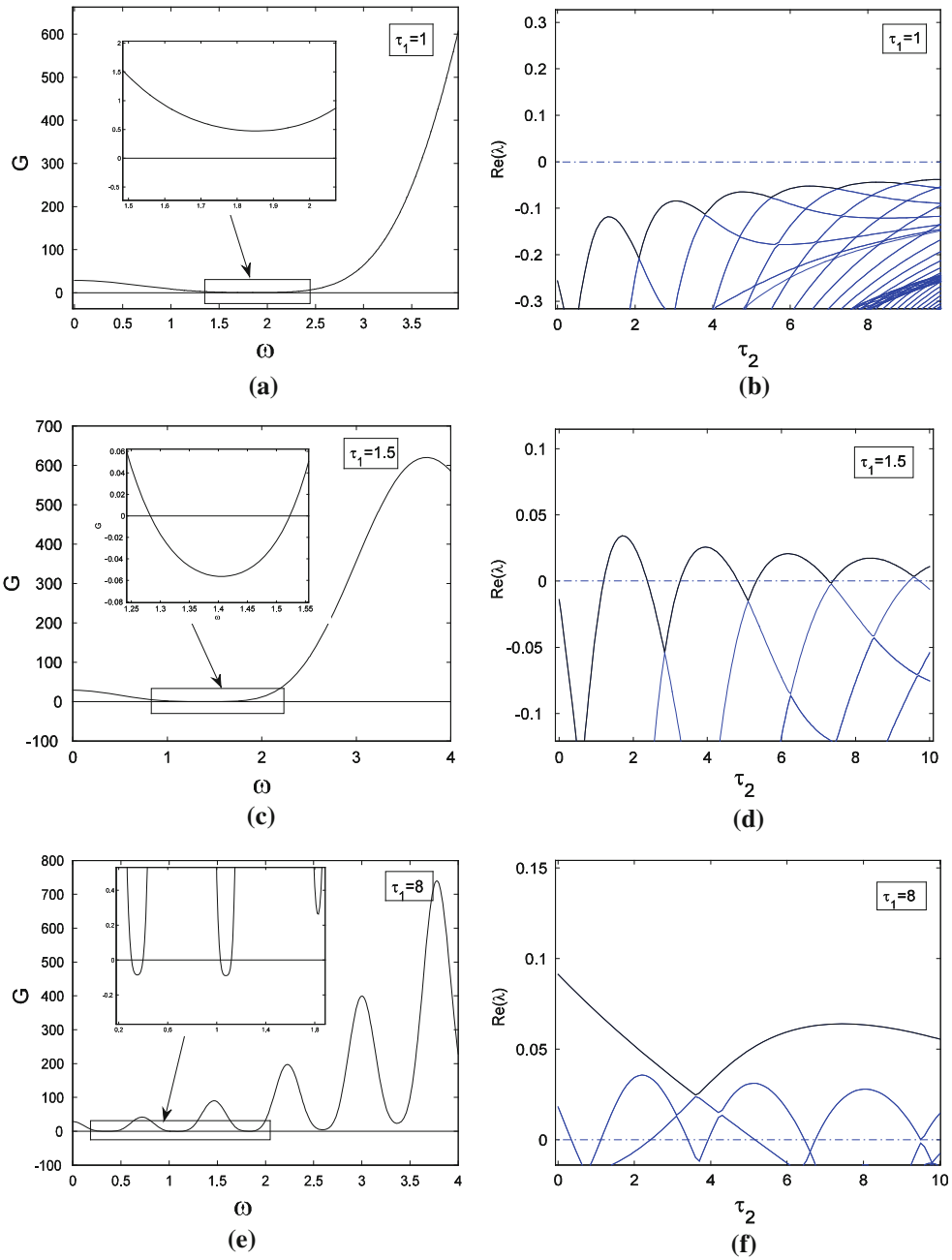

Fig. 1 Roofs of function G (*left column*) and eigenvalue real parts with τ_2 varying (*right column*) for the fixed self-connection delay **a–b** $\tau_1 = 1$, **c–d** $\tau_1 = 1.5$ and **e–f** $\tau_1 = 8$, respectively. The other parameters are chosen as $a_1 = -6$, $a_2 = 2.5$, $a_3 = 2.5$, $a_4 = -6$, $P = 0.4$, $Q = 0.4$

Fig. 1b. The equilibrium point of system (1) is locally asymptotically stable for the arbitrary delay τ_2. With the self-connection delay τ_1 increasing to 1.5, the curve determined by function G moves down and crosses the line $G = 0$. Function G (18) has two positive roots 1.2827 and 1.523, as shown in Fig. 1c. It follows from Fig. 1d that there exist the delay τ_2 intervals in which the eigenvalues have the negative parts. The system dynamics switch from stable to unstable, and then back to stable state with delay τ_2 increasing. It implies that if self-connection delay τ_1 is fixed, we can adjust the neighbor-connection delay τ_2 into the stability regions to suppress system vibration. When delay τ_1 is increased to 8, function G has two pairs of positive roots, as shown in Fig. 1e. However, at this time, the maximum eigenvalue of (5) for the fixed delay $\tau_1 = 0$, i.e. the characteristic equation (6) has positive real part $\mathrm{Re}(\lambda) = 0.0912$. The equilibrium point of system (1) is unstable for any delay τ_2, as shown in Fig. 1f.

To get a deep investigation for the stability switches of equilibrium point, we fix the self-connection delay $\tau_1 = 1.5$. The partial eigenvalues and phase portraits are shown in Figs. 2 and 3 respectively for the different delay τ_2. Figure 2a shows the maximum eigenvalues are a conjugate pair with negative part given by $-0.0295 \pm 1.5705i$, where the

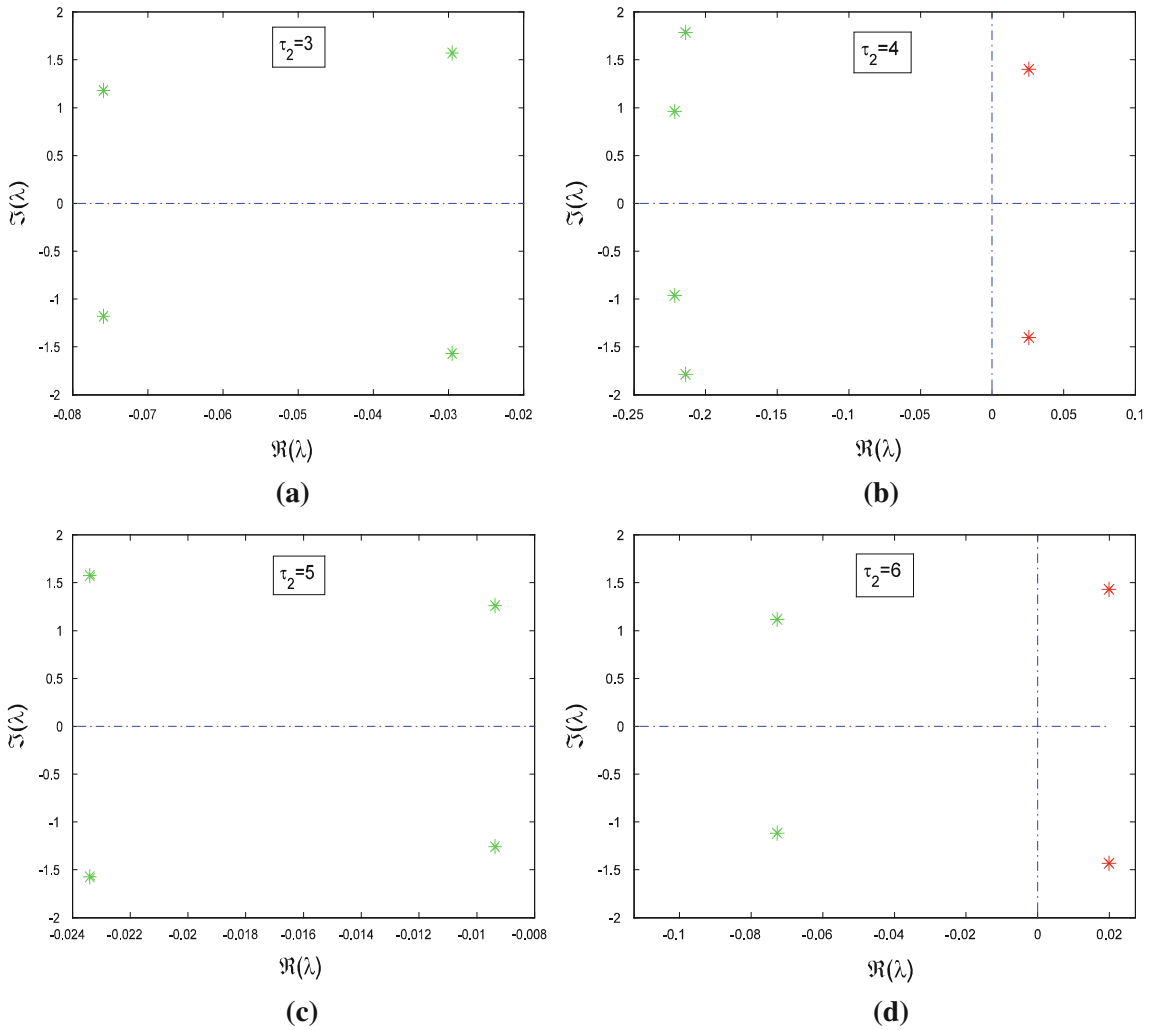

Fig. 2 Distribution of eigenvalues with time delay τ_2 varying **a** $\tau_2 = 3$, **b** $\tau_2 = 4$, **c** $\tau_2 = 5$ and **d** $\tau_2 = 6$ for the fixed parameters $a_1 = -6$, $a_2 = 2.5$, $a_3 = 2.5$, $a_4 = -6$, $P = 0.4$, $Q = 0.4$, $\tau_1 = 1.5$, where the *asterisk* in *green* represents the eigenvalues with negative real part and one with positive real part is in *red color*

neighbor-connection delay is fixed as $\tau_2 = 3$. It implies that the equilibrium point of system (1) is locally asymptotically stable, as shown in Fig. 3a. Letting $\tau_1 = 1.5$ and varying τ_2 yield that the conjugate pair start to pass through the imaginary axis and go into the right-half in the complex plane. For $\tau_2 = 4$, the pair become to be $0.0256 \pm 1.4012i$ shown in Fig. 2b, which suggests that the equilibrium point loses its stability (Fig. 3b). Continuing to increase τ_2, the conjugate pair return and pass through the imaginary axis again. The maximum eigenvalues with negative real parts occurs in the left-hand of complex plane. Figure 2c shows the eigenvalues are $-0.00936 \pm 1.2591i$ for the fixed delay $\tau_2 = 5$. The equilibrium point of system is stabilized again by the neighbor-connection delay τ_2, as shown in Fig. 3c. If the delay τ_2 is fixed as $\tau_2 = 6$, the maximum eigenvalues are conjugate pair with positive part $0.0199 \pm 1.4311i$, as shown in Fig. 2d. The equilibrium point loses its stability again (Fig. 3d). In a word, time delay can lead system to exhibit multi-stable regions. The dynamics of equilibrium point can multi-switch from stable to unstable, and then back to stable state.

Existence of double Hopf bifurcation

It follows from above section that the multiple roots of Eq. (18) can lead system (1) exhibit the phenomenon of stability switches. The dynamical behavior of equilibrium point undergoes the multiple transitions between stability and instability when delays increase and cross the critical delayed values. In this section, we will illustrate these critical values and find the stability regions located in the delayed plane. To this end, the Hopf bifurcation curves represented by delay parameters are investigated. The

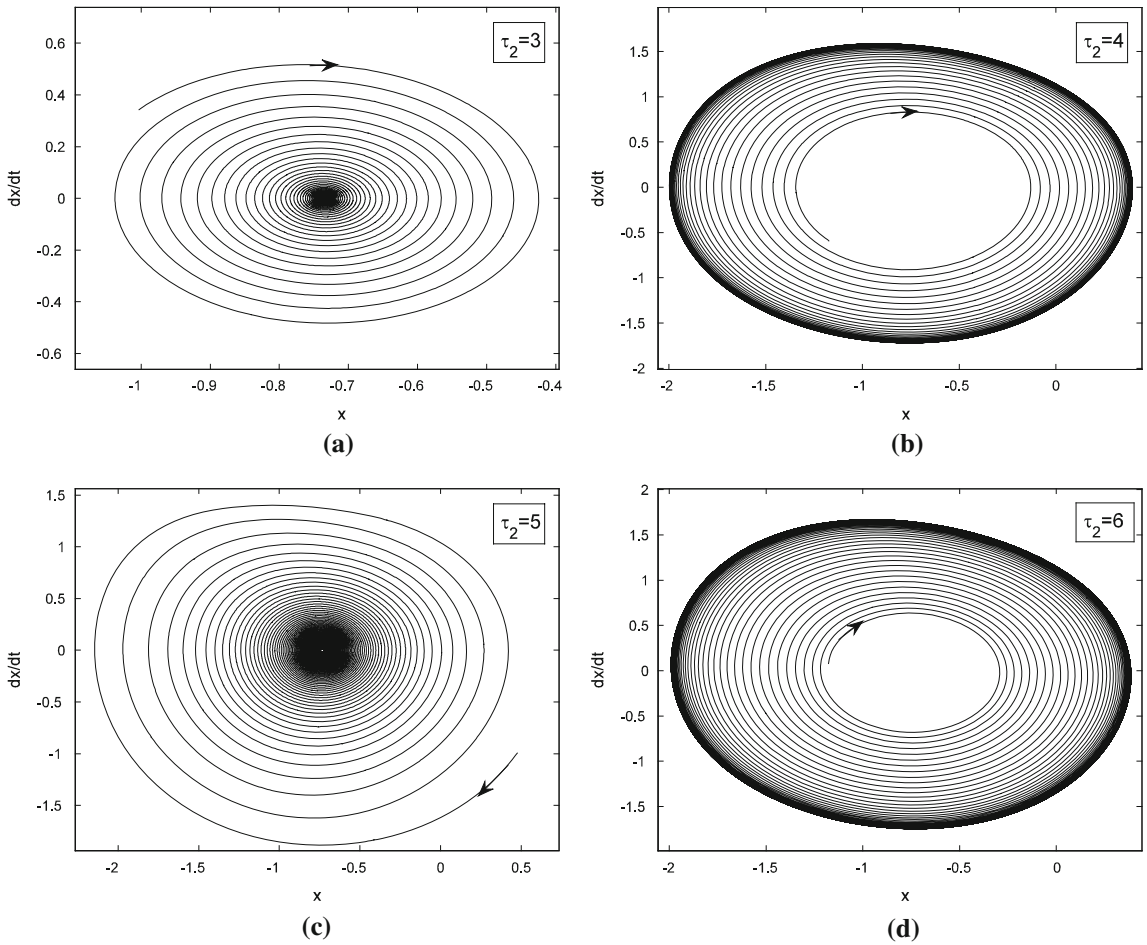

Fig. 3 Phase portraits with time delay τ_2 varying **a** $\tau_2 = 3$, **b** $\tau_2 = 4$, **c** $\tau_2 = 5$ and **d** $\tau_2 = 6$ for the fixed parameters $a_1 = -6$, $a_2 = 2.5$, $a_3 = 2.5$, $a_4 = -6$, $P = 0.4$, $Q = 0.4$, $\tau_1 = 1.5$

coordinate values of the intersection points of these curves are presented, which are the points of the double Hopf bifurcation.

As mentioned above, two pairs of purely imaginary solutions of Eq. (5) are denoted by $\lambda_{1,2} = \pm i\omega_{1,2}$, with $\omega_2 > \omega_1 > 0$. Then two series of the critical delays corresponding to such pairs of purely imaginary eigenvalues are given by

$$\tau_{2,j}^1 = (\varphi_1 + 2j\pi)\omega_1, \quad j = 0, 1, 2, \cdots, \tag{23}$$

where $\varphi_1 \in [0, 2\pi)$,

$$\begin{cases} \cos(2\varphi_1) = \dfrac{1 - \omega_1^2 - (a_1\alpha + a_4\beta)\omega_1 \sin(\omega_1\tau_1)}{a_2a_3\alpha\beta} \\ \quad - \dfrac{(a_1\alpha + a_4\beta)\cos(\omega_1\tau_1) - a_1a_4\alpha\beta\cos(2\omega_1\tau_1)}{a_2a_3\alpha\beta}, \\ \sin(2\varphi_1) = \dfrac{-2\omega_1 + (a_1\alpha + a_4\beta)\omega_1\cos(\omega_1\tau_1)}{a_2a_3\alpha\beta} \\ \quad - \dfrac{(a_1\alpha + a_4\beta)\sin(\omega_1\tau_1) - a_1a_4\alpha\beta\sin(2\omega_1\tau_1)}{a_2a_3\alpha\beta}, \end{cases}$$

and

$$\tau_{2,j}^2 = (\varphi_2 + 2j\pi)/\omega_2, \quad j = 0, 1, 2, \cdots, \tag{24}$$

where $\varphi_2 \in [0, 2\pi)$,

$$\begin{cases} \cos(2\varphi_2) = \dfrac{1 - \omega_2^2 - (a_1\alpha + a_4\beta)\omega_2 \sin(\omega_2\tau_1)}{a_2a_3\alpha\beta} \\ \quad - \dfrac{(a_1\alpha + a_4\beta)\cos(\omega_2\tau_1) - a_1a_4\alpha\beta\cos(2\omega_2\tau_1)}{a_2a_3\alpha\beta}, \\ \sin(2\varphi_2) = \dfrac{-2\omega_2 + (a_1\alpha + a_4\beta)\omega_2\cos(\omega_2\tau_1)}{a_2a_3\alpha\beta} \\ \quad - \dfrac{(a_1\alpha + a_4\beta)\sin(\omega_2\tau_1) - a_1a_4\alpha\beta\sin(2\omega_2\tau_1)}{a_2a_3\alpha\beta}. \end{cases}$$

It follows from (21) that the sign of $\mathrm{Re}(d\lambda/d\tau_2)$ at $\lambda = i\omega_1$, $\tau_2 = \tau_{2,j}^1$ and $\lambda = i\omega_2$, $\tau_2 = \tau_{2,j}^2$ is difficult to determine analytically in terms of the expression of $\omega_{1,2}$. But it can be easily computed numerically. In fact, numerical results show that the quantity of $\mathrm{Re}(d\lambda/d\tau_2)|_{\lambda=i\omega_1}$ is negative and $\mathrm{Re}(d\lambda/d\tau_2)|_{\lambda=i\omega_2}$ is positive. This implies that the

crossing of the imaginary axis is from left to right as τ_2 increases to a certain critical value $\tau^2_{2,j}, j = 0, 1, 2, \cdots$ corresponding to ω_2, and crossing from right to left occurs at a certain values $\tau^1_{2,j}, j = 0, 1, 2, \cdots$ corresponding to ω_2.

For instance, if $\tau^1_{2,0} < \tau^2_{2,0}$ holds for some certain intervals of τ_1, then the unstable equilibrium point becomes stable as τ_2 is increased to cross the critical value $\tau^1_{2,0}$. When τ_2 is further increased to pass through the critical value $\tau^2_{2,0}$, the equilibrium point loses its stability again, where a pair of eigenvalues cross the imaginary axis and arrive to the right half plane. The occurrence and termination of stability switches for the equilibrium point are located at the points of the first and second Hopf bifurcation corresponding ω_1 and ω_2 frequencies, respectively. Similarly, higher order stability regions may be located by $\tau^1_{2,j} < \tau_2 < \tau^2_{2,j}$ for 1, 2, …, resulting in a possibility of multiple stability regions.

Furthermore, the double Hopf bifurcation may occur when the two critical delays are identical, which correspond to the different frequencies ω_1 and ω_2. Geometrically, the double Hopf bifurcation points are the intersections of the first and second Hopf bifurcation curves. Owing to the multiple delays of system (1) considered in the present paper, more complicated expressions have been derived for the critical delays. The possible points of the intersection for the Hopf bifurcation curves cannot be given in a theoretical form. But for a given set of the system parameters, the double Hopf bifurcation points can be solved by the numerical procedure.

As an illustrative example, consider a specific system with the fixed parameters $a_1 = -6$, $a_2 = 2.5$, $a_3 = 2.5$, $a_4 = -6$, $P = 0.4$ and $Q = 0.4$, which are analyzed in section "Linear stability switches". The delays τ_1 and τ_2 are taken as the variable parameters. It follows from (2) that system (1) has only unique equilibrium point given by $(x_0, y_0) = (-0.734629, -0.734629)$. The frequencies of the first and second Hopf bifurcation can be obtained in terms of (18) for each fixed value of delay τ_1. For example, chosen time delay as $\tau_1 = 1.8$, one has the frequencies $\omega_1 = 1.0773$ and $\omega_2 = 1.3697$, respectively. The equilibrium point switches to stable state τ_2 when increases to $\tau^1_{2,0} = 0.256977$ corresponding to the first Hopf bifurcation, and remains its stability until τ_2 reaches $\tau^2_{2,0} = 1.11253$ relating to the second Hopf bifurcation. Similarly, the equilibrium point is locally asymptotically stable if the delay is fixed into the range of $(\tau^1_{2,1}, \tau^2_{2,1}) = (3.1730, 3.4065)$, which is the second order stability region. In such a way, the equilibrium point switches its stability and instability a finite number of times. For each fixed delay τ_1, based on (23) and (24), a series of critical curves of the stability regions can be exhibited in the (τ_1, τ_2) parameter plane, as shown in Fig. 4. These curves divide the parameter plane into several stable and unstable regions. The stability regions are indicated by $S_j, j = 0, 1, 2, \cdots$, where j stands for the order of the stability regions.

It follows from Fig. 4 that the curves of the first and second Hopf bifurcation intersect at the point $(\tau^c_1, \tau^c_2) = (2.8467, 1.1767)$. The frequencies corresponding to the Hopf bifurcation are respectively $\omega_1 = 0.7314$ and $\omega_2 = 0.9735$, as shown in Fig. 5. It implies that the intersection point is a non-resonate double Hopf bifurcation, which is usually referred as the codimension-two bifurcation. This singularity point is a source of more complicated dynamics, such as the stable quasi-periodic behavior and unstable solution. Similarly, the higher order double Hopf bifurcation points and the corresponding frequencies can be obtained in the (τ_1, τ_2) parameter plane, which are shown in Fig. 4 and Table 1.

Central manifold reduction

It follows from the previous section that multiple delays of system (1) induce two different values of frequencies corresponding to the first and second Hopf bifurcation. The existence of a double Hopf bifurcation can be detected by the local stability analysis. The intersections of these Hopf bifurcation curves are the double Hopf bifurcation points. In this section, we represent the typical dynamical behaviors and the bifurcation sets in the neighborhood of the double Hopf bifurcation point by means of the central manifold reduction and normal form method (Buono and Belair 2003; Faria and Magalhaes 1995a, b). The periodic solutions corresponding to the different frequencies and the stable quasi-periodic solutions resulting from the double

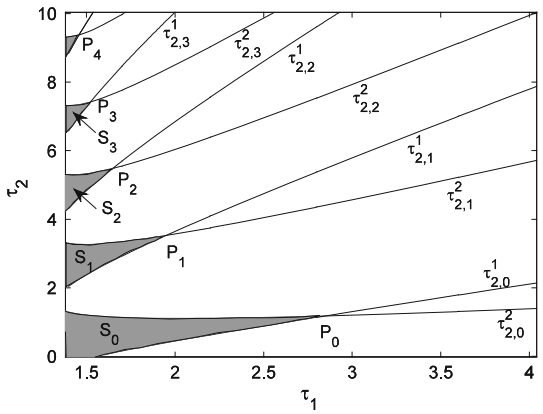

Fig. 4 Variation of the critical delay values τ_2 with τ_1 in the (τ_1, τ_2) parameter plane for the fixed parameters as $a_1 = -6$, $a_2 = 2.5$, $a_3 = 2.5$, $a_4 = -6$, $P = 0.4$ and $Q = 0.4$, respectively, where $S_j, j = 0, 1, 2, \cdots$ denote the stability regions of equilibrium point (x_0, y_0) and P_j, $j = 0, 1, 2, \ldots$ are the double Hopf bifurcation points

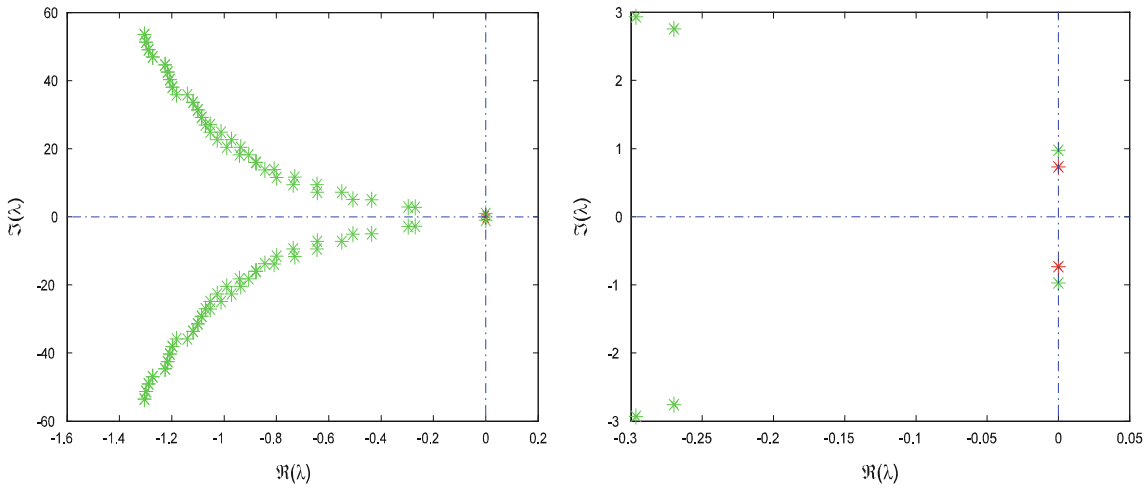

Fig. 5 **a** Roots of the characteristic equation in the complex plane for $(\tau_1^c, \tau_2^c) = (2.8467, 1.1767)$ and **b** enlargement near (0, 0) corresponding to **a**, where the other parameters are fixed as $a_1 = -6$, $a_2 = 2.5$, $a_3 = 2.5$, $a_4 = -6$, $P = 0.4$, $Q = 0.4$

Table 1 Coordinate values of the double Hopf bifurcation points and the corresponding frequencies

(τ_1^c, τ_2^c)	ω_1	ω_2
(2.8467, 1.1767)	0.7314	0.9735
(1.9473, 3.5226)	1.0052	1.2985
(1.6481, 5.4804)	1.1682	1.4474
(1.5225, 7.4198)	1.2630	1.5121
(1.4584, 9.3768)	1.3222	1.5422

Hopf bifurcations point are investigated in the system under consideration. Introducing the transformation $t \to t/\tau_1$ yields that system (1) becomes

$$\begin{cases} \dfrac{dx(t)}{dt} = \tau_1[-x(t) + a_1 S(x(t-1)) + a_2 S(y(t-r)) + P], \\ \dfrac{dy(t)}{dt} = \tau_1[-y(t) + a_3 S(x(t-r)) + a_4 S(y(t-1)) + Q], \end{cases} \tag{25}$$

where $r = \tau_2/\tau_1$. For the rescale system defined by system (25), the two Hopf bifurcation frequencies, namely ω_{01} and ω_{02}, are now given by $\omega_{01} = \tau_1\omega_1$ and $\omega_{02} = \tau_1\omega_2$, respectively. Setting $x(t) \to x(t) - x_0$ and $y(t) \to y(t) - y_0$ yields that system (25) can be rewritten as system (26).

Regarding the time delays τ_1 and r as the bifurcation parameters, we let

$$\tau_1 = \tau_1^c + \varepsilon\delta_1, \quad r = r^c + \varepsilon\delta_2,$$

where $r^c = \tau_2^c/\tau_1^c$ and $\varepsilon\delta_1, \varepsilon\delta_2$ are the unfolding parameters.

$$\begin{cases} \dfrac{dx(t)}{dt} = -\tau_1 x(t) + a_1\tau_1\left(S'(x_0)x(t-1) + \dfrac{1}{2}S''(x_0)x^2(t-1) + \dfrac{1}{6}S'''(x_0)x^3(t-1)\right) \\ \qquad\qquad + a_2\tau_1\left(S'(y_0)y(t-r) + \dfrac{1}{2}S''(y_0)y^2(t-r) + \dfrac{1}{6}S'''(y_0)y^3(t-r)\right), \\ \dfrac{dy(t)}{dt} = -\tau_1 y(t) + a_3\tau_1\left(S'(x_0)x(t-r) + \dfrac{1}{2}S''(x_0)x^2(t-r) + \dfrac{1}{6}S'''(x_0)x^3(t-r)\right) \\ \qquad\qquad + a_4\tau_1\left(S'(y_0)y(t-1) + \dfrac{1}{2}S''(y_0)y^2(t-1) + \dfrac{1}{6}S'''(y_0)y^3(t-1)\right). \end{cases} \tag{26}$$

It follows that

$$\begin{aligned} \tau_2 &= \tau_1 r = (\tau_1^c + \varepsilon\delta_1)(r^c + \varepsilon\delta_2) \\ &= \tau_2^c + \varepsilon(r^c\delta_1 + \tau_1^c\delta_2) + o(\varepsilon). \end{aligned} \tag{27}$$

Then system (25) becomes

$$\begin{cases} \dfrac{dx(t)}{dt} = \left(\tau_1^c + \varepsilon\delta_1\right)\left(-x(t) + a_1\left(S'(x_0)x(t-1) + \dfrac{1}{2}S''(x_0)x^2(t-1) + \dfrac{1}{6}S'''(x_0)x^3(t-1)\right)\right) \\ \qquad + a_2\left(\tau_1^c + \varepsilon\delta_1\right)\left(S'(y_0)y(t-r^c-\varepsilon\delta_2) + \dfrac{1}{2}S''(y_0)y^2(t-r^c-\varepsilon\delta_2)\right) \\ \qquad + \dfrac{1}{6}a_2\left(\tau_1^c + \varepsilon\delta_1\right)S'''(y_0)y^3(t-r^c-\varepsilon\delta_2) + \cdots, \\ \dfrac{dy(t)}{dt} = \left(\tau_1^c + \varepsilon\delta_1\right)\left(-y(t) + a_3\left(S'(x_0)x(t-r^c-\varepsilon\delta_2) + \dfrac{1}{2}S''(x_0)x^2(t-r^c-\varepsilon\delta_2)\right)\right) \\ \qquad + a_4\left(\tau_1^c + \varepsilon\delta_1\right)\left(S'(y_0)y(t-1) + \dfrac{1}{2}S''(y_0)y^2(t-1) + \dfrac{1}{6}S'''(y_0)y^3(t-1)\right) \\ \qquad + \dfrac{1}{6}a_3\left(\tau_1^c + \varepsilon\delta_1\right)S'''(x_0)x^3(t-r^c-\varepsilon\delta_2) + \cdots. \end{cases} \tag{28}$$

To apply the central manifold reduction, it is necessary to changes system (28) into a functional differential equation (Hale 1977). Let $C \triangleq C([-\tau, 0], R^2)$ as the Banach space of continuous functions from $[-\tau, 0]$ to R^2 with the supremum norm, where $\tau = \max\{1, r\}$. For any $\phi \in C$, we define

$$L_1(\varepsilon)\phi = \int_{-\tau}^{0} [d\eta_1(\theta, \varepsilon)]\phi(\theta), \tag{31}$$

where

$$d\eta_1(\theta, \varepsilon) = \varepsilon\delta_1\begin{pmatrix} -\delta(\theta) + a_1\tau_1^c S''(x_0)\delta(\theta+1) & b_1 \\ b_2 & -\delta(\theta) + a_4\tau_1^c S''(y_0)\delta(\theta+1) \end{pmatrix}d\theta, \tag{32}$$

$$L(0)\phi = \int_{-\tau}^{0} [d\eta(\theta)]\phi(\theta), \tag{29}$$

where $\eta : [-\tau, 0] \to R^2 \times R^2$ is a real-valued function of bounded variation in $[-\tau, 0]$ with

$$d\eta(\theta) = \tau_1^c\begin{pmatrix} -\delta(\theta) + a_1\alpha\delta(\theta+1) & a_2\beta\delta(\theta+r^c) \\ a_3\alpha\delta(\theta+r^c) & -\delta(\theta) + a_4\beta\delta(\theta+1) \end{pmatrix}d\theta, \tag{30}$$

where $\alpha = S'(x_0)$, $\beta = S'(y_0)$, and $\delta(\theta)$ is Dirac function. Further, we define

and

$$b_1 = a_2 S''(y_0)\left((\tau_1^c + \varepsilon\delta_1)\delta(\theta + r^c + \varepsilon\delta_2) - \tau_1^c\delta(\theta + r^c)\right),$$

$$b_2 = a_3 S''(x_0)\left((\tau_1^c + \varepsilon\delta_1)\delta(\theta + r^c + \varepsilon\delta_2) - \tau_1^c\delta(\theta + r^c)\right).$$

For $\phi \in C$, the linear operator defined by system (28) generates an infinitesimal generator of the semi-flow of bounded linear operators with

$$A(0)\phi = \begin{cases} \dfrac{d\phi(\theta)}{d\theta} & \theta \in [-\tau, 0), \\ L(0)\phi & \theta = 0, \end{cases} \tag{33}$$

and

$$A_1(\varepsilon)\phi = \begin{cases} 0 & \theta \in [-\tau, 0), \\ L_1(\varepsilon)\phi & \theta = 0. \end{cases} \tag{34}$$

Set

$$N\phi = \begin{cases} 0 & \theta \in [-\tau, 0), \\ F(\phi_1, \phi_2) & \theta = 0, \end{cases} \tag{35}$$

where

$$F(\phi_1, \phi_2) = \begin{Bmatrix} F_1(\phi_1, \phi_2) \\ F_2(\phi_1, \phi_2) \end{Bmatrix}, \tag{36}$$

and

$$\begin{aligned} F_1(\phi_1, \phi_2) = {} & (\tau_1^c + \varepsilon\delta_1)a_1\left(\frac{1}{2}S''(x_0)\phi_1^2(-1) + \frac{1}{6}S'''(x_0)\phi_1^3(-1)\right) \\ & + a_2(\tau_1^c + \varepsilon\delta_1)\left(\frac{1}{2}S''(y_0)\phi_2^2(-r^c - \varepsilon\delta_2)\right. \\ & \left. + \frac{1}{6}S'''(y_0)\phi_2^3(-r^c - \varepsilon\delta_2)\right), \end{aligned}$$

$$\begin{aligned} F_2(\phi_1, \phi_2) = {} & (\tau_1^c + \varepsilon\delta_1)a_3\left(\frac{1}{2}S''(x_0)\phi_1^2(-r^c - \varepsilon\delta_2)\right. \\ & \left. + \frac{1}{6}S'''(x_0)\phi_1^3(-r^c - \varepsilon\delta_2)\right) + (\tau_1^c + \varepsilon\delta_1) \\ & a_4\left(\frac{1}{2}S''(y_0)\phi_2^2(-1) + \frac{1}{6}S'''(y_0)\phi_3^3(-1)\right). \end{aligned}$$

Thus, system (28) becomes

$$\dot{v}_t = A(0)v_t + A_1(\varepsilon)v_t + Nv_t \tag{37}$$

where $v = (v_1,\ v_2)^{\mathrm{T}}, v_t(\theta) = v(t+\theta),\ -\tau \le \theta \le 0$. For $\psi \in C^* = C([0,\tau], R^2)$, the adjoint operators $A^*(0)$ and $A_1^*(\varepsilon)$ of $A(0)$ and $A_1(\varepsilon)$, respectively, are given by

$$A^*(0)\psi(s) = \begin{cases} \frac{d\psi(s)}{ds} & s \in (0,\tau], \\ \int_{-\tau}^{0} d\eta^{\mathrm{T}}(s)\psi(-s) & s = 0, \end{cases} \tag{38}$$

and

$$A_1^*(\varepsilon)\psi(s) = \begin{cases} 0 & s \in (0,\tau], \\ \int_{-\tau}^{0} d\eta^{\mathrm{T}}(s,\varepsilon)\psi(-s) & s = 0 \end{cases} \tag{39}$$

For $\varphi \in C$ and $\psi \in C^*$, we introduce the bilinear form

$$\begin{aligned} \langle \psi(s), \varphi(\theta)\rangle = {} & \bar{\psi}^{\mathrm{T}}(0)\varphi(0) \\ & - \int_{-\tau}^{0}\int_{\xi=0}^{\theta} \bar{\psi}^{\mathrm{T}}(\xi - \theta)d\eta(\theta)\varphi(\xi)d\xi. \end{aligned} \tag{40}$$

From the above discussion, we know that system (25) has two pairs of purely imaginary eigenvalues $\Lambda = \{\pm i\omega_{01}, \pm i\omega_{02}\}$ and the other eigenvalues with negative real parts at the double Hopf bifurcation point. Therefore, the Banach space C can be split into two subspaces as $C = \mathrm{P}_\Lambda \oplus \mathrm{Q}_\Lambda$, where P_Λ is the four-dimensional center subspace spanned by the basic vectors of the linear operator $A(0)$ associated with the imaginary characteristic roots, and Q_Λ is the complement subspace of P_Λ (Faria and Magalhaes 1995a, b). Now, We suppose $q_j(\theta)$ and $q_j^*(\theta)$ are the eigenvectors of $A(0)$ and $A^*(0)$, respectively, corresponding to eigenvalue $i\omega_{0j}$ and $-i\omega_{0j}$, $j = 1, 2$, i.e. $A(0)q_j(\theta) = i\omega_{0j}q_j(\theta)$, and $A^*(0)q_j^*(s) = -i\omega_{0j}q_j^*(s)$. By the direct computation, we have

$$q_j(\theta) = (\,1 \quad \alpha_j\,)^{\mathrm{T}} e^{i\omega_{0j}\theta}, \quad \text{and} \quad q_j^*(s) = \bar{K}_j(\,\beta_j \quad 1\,)^{\mathrm{T}} e^{i\omega_{0j}s},$$

where

$$\alpha_j = \frac{(e^{i\omega_{0j}} - a_1\alpha)e^{-i\omega_{0j}+i\tau\omega_{0j}} + ie^{i\tau\omega_{0j}}\omega_{0j}}{a_2\beta},$$

$$\beta_j = -\frac{a_3\alpha e^{i\tau\omega_{0j}}}{-1 + a_1\alpha e^{i\omega_{0j}} + i\omega_{0j}},$$

$$\begin{aligned} \frac{1}{K_j} = {} & 2a_3\alpha\tau e^{-i\tau\omega_{0j}} + \frac{a_3\alpha e^{i\tau\omega_{0j}}(e^{i\omega_{0j}} + a_1\alpha)}{e^{i\omega_{0j}}(1 + i\omega_{0j}) - a_1\alpha} \\ & + \frac{e^{i(\tau-2)\omega_{0j}}(e^{i\omega_{0j}} + a_4\beta)(e^{i\omega_{0j}}(1 + i\omega_{0j}) - a_1\alpha)}{a_2\beta}. \end{aligned}$$

Furthermore, it follows that the real bases for P_Λ and its dual space can be expressed as (Chen and Yu 2006)

$$\begin{aligned} \Phi(\theta) &= \left(\phi^1, \phi^2, \phi^3, \phi^4\right) \\ &= \sqrt{2}(\mathrm{Re}(q_1(\theta)), \mathrm{Im}(q_1(\theta)), \mathrm{Re}(q_2(\theta)), \mathrm{Im}(q_2(\theta))), \end{aligned} \tag{41}$$

and

$$\begin{aligned} \Psi(s) &= \left(\psi^1, \psi^2, \psi^3, \psi^4\right)^{\mathrm{T}} \\ &= \sqrt{2}\left(\mathrm{Re}\left(q_1^*(\theta)\right), \mathrm{Im}\left(q_1^*(\theta)\right), \mathrm{Re}\left(q_2^*(\theta)\right), \mathrm{Im}\left(q_2^*(\theta)\right)\right)^{\mathrm{T}}, \end{aligned} \tag{42}$$

respectively. Note that the factor $\sqrt{2}$ is required for normalizing the linear part of transformed equation. It is easily verified that $\left\langle q_j^*, q_j \right\rangle = 1$ and $\left\langle q_j^*, \bar{q}_j \right\rangle = 0$, where $j = 1, 2$ and

$$\langle \Psi, A(0)\Phi \rangle = B = \begin{pmatrix} 0 & \omega_{01} & 0 & 0 \\ -\omega_{01} & 0 & 0 & 0 \\ 0 & 0 & 0 & \omega_{02} \\ 0 & 0 & -\omega_{02} & 0 \end{pmatrix}. \tag{43}$$

Define

$$u = (u_1, u_2, u_3, u_4)^T = \langle \Psi, v_t \rangle, \tag{44}$$

which actually represents the local coordinate system on the four-dimensional center manifold, induced by the basis

Ψ. It follows (41) and (42) that one can decompose v_i into two parts given by

$$v_t = v_t^{P_\Lambda} + v_t^{Q_\Lambda} = \Phi\langle\Psi, v_t\rangle + v_t^{Q_\Lambda} = \Phi u + v_t^{Q_\Lambda}, \tag{45}$$

which implies that Φu is the projection of v_i on the center manifold. Substituting (45) into (37) and applying the bilinear operator (37) with Ψ given by (37) to the resulting equation yields

$$\left\langle \Psi, \left(\Phi\dot{u} + \dot{v}_t^{Q_\Lambda}\right)\right\rangle = \left\langle \Psi, (A(0) + A_1(\varepsilon) + N)\left(\Phi u + v_t^{Q_\Lambda}\right)\right\rangle. \tag{46}$$

With the aid of (45), one obtains

$$\begin{aligned}\langle\Psi, \Phi\rangle\dot{u} =& \langle\Psi, A(0)\Phi\rangle u + \langle\Psi, A_1(\varepsilon)\Phi\rangle u + \langle\Psi, N\Phi u\rangle \\ \Rightarrow\ & \dot{u} = Bu + \Psi(0)F(t, \Phi u).\end{aligned} \tag{47}$$

where B is determined by (43). It should be noted that $\varepsilon\delta_1$ and $\varepsilon\delta_2$ are very small in the neighborhood of $(\tau_1^c,\ \tau_2^c)$. This implies that

$$\sin(\varepsilon\delta_1\omega_1) \sim \varepsilon\delta_1\omega_1, \cos(\varepsilon\delta_1\omega_1) \sim 1, \sin(\varepsilon\delta_2\omega_2) \sim \varepsilon\delta_2\omega_2,$$
$$\cos(\varepsilon\delta_2\omega_2) \sim 1.$$

Executing the standard normalization technique as (Xu and Pei 2008; Buono and Belair 2003), one obtains the amplitude equation coming from the polar normal form of the central manifold system given by (Guckhenheimerm and Holmes 1983)

$$\begin{cases} \dot{r}_1 = \mu_1 r_1 + a_{11} r_1^3 + a_{12} r_1 r_2^2, \\ \dot{r}_2 = \mu_2 r_2 + a_{21} r_1^2 r_2 + a_{22} r_2^3. \end{cases} \tag{48}$$

As mentioned above, chosen the system parameters as $a_1 = -6,\ a_2 = 2.5,\ a_3 = 2.5,\ a_4 = -6,\ P = 0.4,\ Q = 0.4$, the double Hopf bifurcation points are illustrated in Fig. 4 and Table 1. For convenience, we only investigate the first order critical delayed value of the double Hopf bifurcation given by $\tau_1^c = 2.8467, \tau_2^c = 1.1767$. The same procedure can be applied to the other points. Substituting the parameter values into system (48), one obtains the corresponding coefficients given by $\mu_1 = 0.176689\varepsilon\delta_1 - 0.437895\varepsilon\delta_2,\ \mu_2 = -0.154889\varepsilon\delta_1 + 0.518251\varepsilon\delta_2,\ a_{11} = -2.24354,\ a_{12} = -4.56238,\ a_{21} = -0.439421,\ a_{22} = -5.240934$, respectively. From the dynamical theory (Guckhenheimerm and Holmes 1983), the curves of the secondary bifurcation are represented as $T_1 = \{(\mu_1, \mu_2) : \mu_1 = 0.870528\mu_2 + O(\mu_2^2),\ \mu_2 > 0\}$ and $T_2 = \{(\mu_1, \mu_2) : \mu_2 = 0.195861\mu_1 + O(\mu_1^2), \mu_1 > 0\}$ in the (μ_1, μ_2) plane. To analyze the dynamical behaviors of system (1) in parameter (τ_1, τ_2) plane, the bifurcation curves in terms of τ_1 and τ_2 can be obtained by virtue of (27). The dynamical classification near the first order point of double Hopf bifurcation is shown in Fig. 6, which is called the two-parameter bifurcation diagram. It should be noticed that the fixed point with $r_1 = r_2 = 0$ in system (48) corresponds to the equilibrium point of the origin system. Possible fixed point in the invariant coordinate axes for (48) with $r_1 = 0$ or $r_2 = 0$ correspond to limit cycle of the origin system, while a nontrivial fixed point with $r_1 > 0$ and $r_2 > 0$ generates a two-dimensional tours (quasi-periodic solution with two incommensurate frequencies). The stability of all these solutions in the original system is clearly detectable from that of the corresponding object in (48), as shown in Fig. 6.

Numerical simulations

To illustrate the theoretical works of determining the double Hopf bifurcation properties, in this section, we present some numerical simulation to verify the system solutions. As mentioned above, we kept on choosing the parameters as $a_1 = -6,\ a_2 = 2.5,\ a_3 = 2.5,\ a_4 = -6,\ P = 0.4$ and $Q = 0.4$, respectively. The time delays τ_1 and τ_2 are considered as the variable parameters. Fig. 7 shows the one-parameter bifurcation diagrams with varying delay τ_2 for fixed delay τ_1. Phase portraits of the typical behaviors near the double Hopf bifurcation point are illustrated in Fig. 8, respectively.

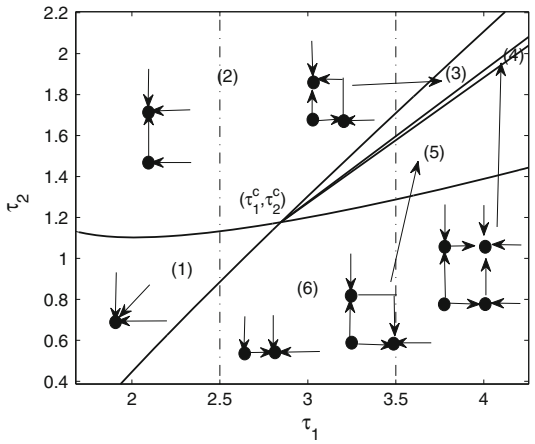

Fig. 6 Classification and bifurcation sets for system (1) near the first order point of the double Hopf bifurcations $(\tau_1^c, \tau_2^c) = (2.8467, 1.1767)$ in the parameter (τ_1, τ_2) plane. The other parameters are chosen at the same as those in Fig. 4

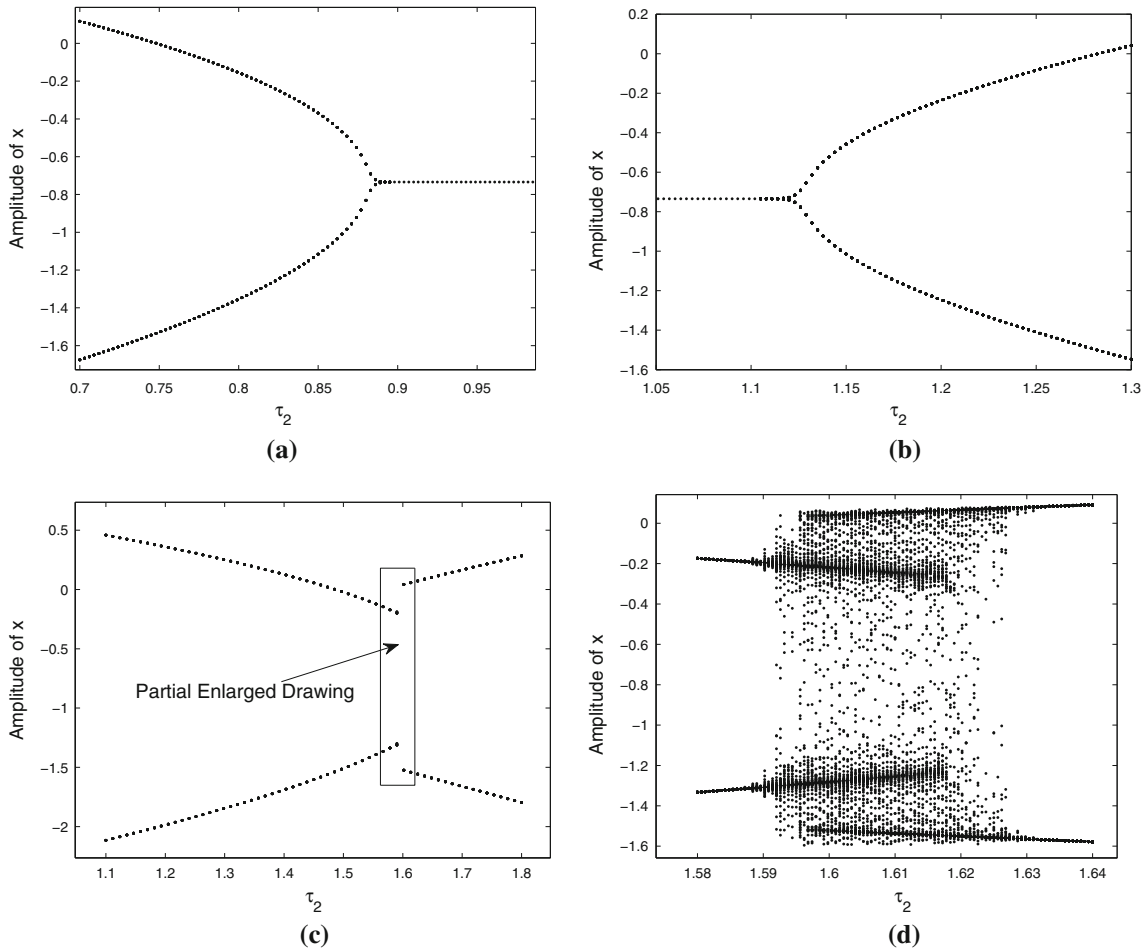

Fig. 7 One-parameter bifurcation diagram with varying the delay τ_2 for **a** $\tau_1 = 2.5$, $\tau_2 \in [0.7,1]$, **b** $\tau_1 = 2.5$, $\tau_2 \in [1.05, 1.3]$, **c** $\tau_1 = 3.5$, $\tau_2 \in [1.1, 1.8]$, and **d** the partial enlargement of the **c** box, respectively. The other parameters are chosen at the same as those in Fig. 4

Firstly, two delays are fixed as $(\tau_1, \tau_2) = (2.5, 1.0)$ located in region 1 of Fig. 6. The numerical solution of system (1) is shown in Fig. 8a. The trajectory asymptotically converges to the equilibrium point $(x_0, y_0) = (-0.734629, -0.734629)$. It implies the point is locally asymptotically stable. With the increasing of delay τ_2, the equilibrium point loses its stability in term of the supercritical Hopf bifurcation, where the parameters encounter the second Hopf bifurcation curve and enter region 2 of Fig. 6. The system periodically oscillates with the second frequency, as shown in Fig. 8b. The one-parameter bifurcation diagram with increasing τ_2 is shown in Fig. 7b. The oscillation amplitude of system is increasing with delay τ_2 varying. However, when delay τ_2 is decreased from region 1 of Fig. 6, the parameters will encounter the first Hopf bifurcation curve related to ω_1 frequency. This implies that the equilibrium point loses its stability through a reverse Hopf bifurcation, as shown in Fig. 7a. It follows that this bifurcation is also supercritical Hopf bifurcation. The system is exhibited the oscillation solution with ω_1 frequency as it enters into region 6, as shown in Fig. 8f.

Furthermore, when we choose delay $\tau_1 = 3.5$, the one-parameter bifurcation diagram with varying τ_2 is shown in Fig. 7c, where Fig. 7d is the partial enlargement of the box in Fig. 7c. Figure 8c and e respectively show the stable state of periodical solutions with the different frequencies. With delay τ_2 varying from region 3–4, the stable periodic solution loses its stability through the Neimark-Sacker bifurcation. It suggests that the system behavior moves to a two-frequency quasi-periodic state, as shown in Fig. 8d. The phase portrait clearly shows the modulation of the peak intensities, which is also called as 2-torus. Keeping delay τ_2 vary, when parameters encounter and cross the other secondary bifurcation, the system behavior transforms into the periodic activity again from the 2-torus solution. The analytical predictions of system solutions are good representatives of the numerical results.

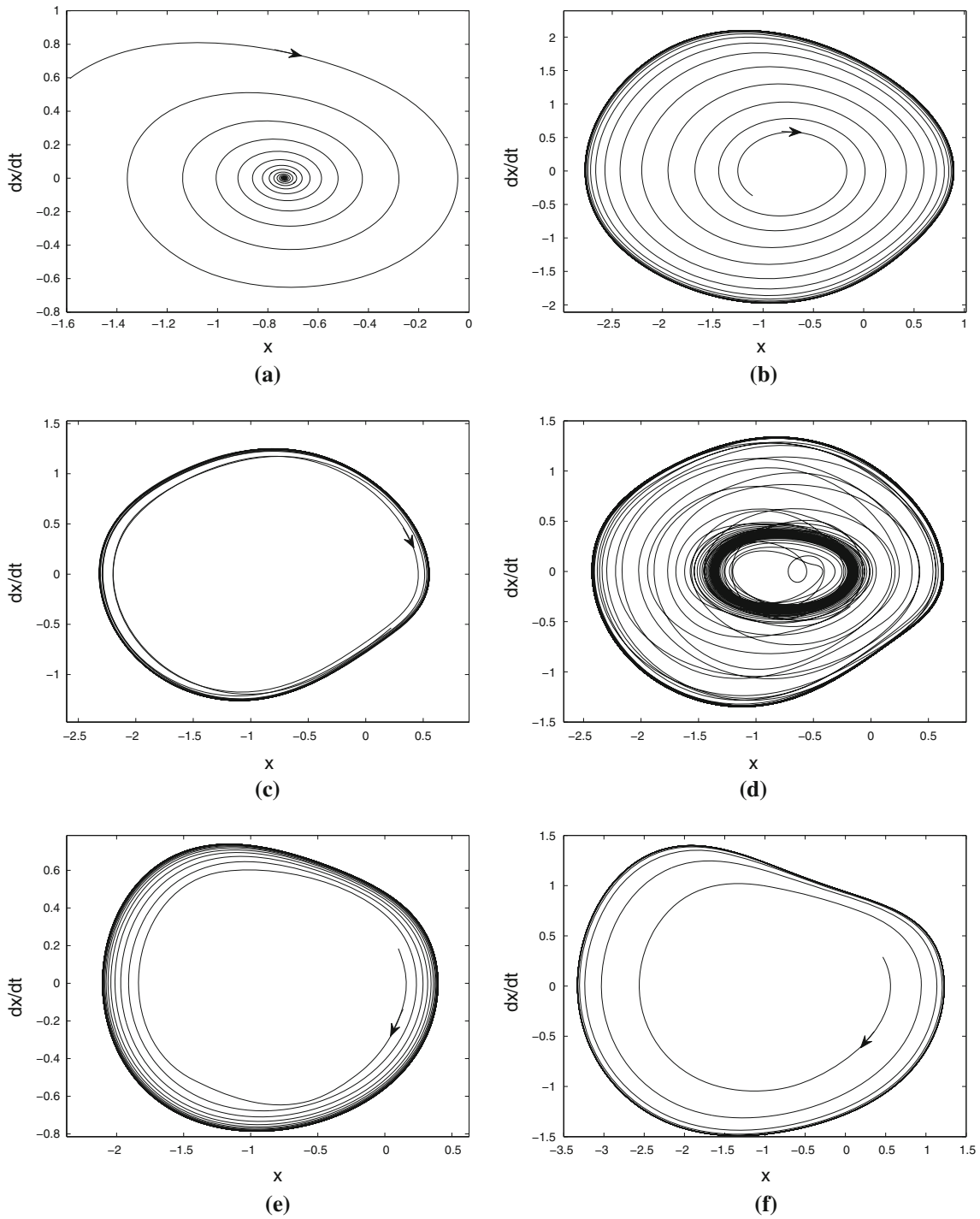

Fig. 8 Phase portraits of the numerical simulation for the dynamical behavior in system (1) near the first order point of the double Hopf bifurcation, where (τ_1, τ_2) is fixed as **a** (2.0, 0.8), **b** (2.5, 1.6), **c** (3.5, 1.6), **d** (3.5, 1.64), **e** (3.5, 1.4), and **f** (3.5, 0.8), respectively. The other parameters are chosen at the same as those in Fig. 4

Conclusion

In neural system, action potential plays a crucial role in many information communications. To understand the information representation, many mathematical models are proposed and the mechanism of information processing is investigated by using the analytical method of nonlinear dynamics. The quiescent state, periodic spiking, quasi-periodic behavior and bursting activity are all the important biological behavior with the different neuro-computational

properties (Song and Xu 2012a; 2012b). The action potential exhibits the quasi-periodic behavior when the number of incommensurable frequencies is finite, which is called the multi-frequency rhythmic activity. Their power spectra are discrete with peaks corresponding to the composed frequencies (Izhikevich 1999). In fact, EEG recordings of brain can demonstrate the rhythmic activity with a few pronounced frequencies. For example, the most prominent are gamma (30–100 Hz) oscillations in the cortex and theta (4–8 Hz) oscillations in the hippocampus (Llinas 1988). Recently, Marichal et al. (2010) considered the dynamic behavior of a quasi-periodic orbit obtained by the Neimark-Sacker bifurcation in a simple discrete recurrent neural network model.

It is well known that time delay is an inevitable factor in the signal transmission between biological neurons or electronic-model-neurons. Neural systems with time delays have very rich dynamical behaviors. In this paper, a neural network with two different types of delays involved in self- and neighbor-connection has been studied. The occurrence of the multiple delays greatly complicates the analysis of stability and bifurcation. The stability regions are strongly relied on time delays. For the different values of delays, the system may exhibit the different parameter regions involved in the delay-independence stability and delay-dependence stability. In special, when the characteristic equation of the system has multiple roots, there exists the delay window, where the equilibrium point is either locally asymptotically stable. To illustrate these critical values and find the stability regions, the Hopf bifurcation curves are illustrated. The multiple stability regions are obtained in the delayed parameter plane. The transverse direction of the imaginary eigenvalues located at the critical values is determined by means of the numerical computation.

Furthermore, the system exhibits the double Hopf bifurcation points due to the two pairs of imaginary eigenvalues appearing on the margin of stability regions simultaneously. Considering the multiple delays as the bifurcation parameters, the classification of the various dynamic behaviors in the neighborhood of the double Hopf bifurcation point is obtained in detail in term of the central manifold reduction and normal form method. The system may exhibit the equilibrium solution, periodic solutions with the different frequencies of the first and second Hopf bifurcations, and quasi-periodic solutions. In addition, the quasi-periodic solution is obtained by the Neimark- Sacker bifurcation of the periodic solutions. Numerical results are given to illustrate that the double Hopf bifurcation is an interaction of the supercritical–supercritical Hopf bifurcations. Finally, the one-parameter bifurcation diagrams and phase portraits verify the agreement between the theoretical analysis and numerical simulations.

Acknowledgments This research is supported by the State Key Program of National Natural Science of China under Grant No. 11032009, Shanghai Leading Academic Discipline Project in No. B302, the PhD Start-up Fund of Shanghai Ocean University in No. A-2400-11-0214 and Young Teacher Training Program of Colleges and Universities in Shanghai under Grant No. ZZhy12030.

References

Bélair J, Campbell SA (1994) Stability and bifurcations of equilibrium in multiple-delayed differential equation. SIAM J Appl Math 54(5):1402–1424

Budak E (2003) An analytical design method for milling cutters with nonconstant pitch to increase stability, part I: theory. ASME J Manuf Sci Eng 125(1):29–35

Buono PL, Belair J (2003) Restrictions and unfolding of double Hopf bifurcation in functional differential equations. J Differ Equ 189(1):234–266

Campbell SA (2007) Time delays in neural systems. In: McIntosh AR, Jirsa VK (eds) Handbook of brain connectivity. Springer, Berlin, p 65

Campbell SA, Ncube I, Wu J (2006) Multistability and stable asynchronous periodic oscillations in a multiple-delayed neural system. Physica D 214(2):101–119

Cao J, Xiao M (2007) Stability and Hopf bifurcation in a simplified BAM neural network with two time delays. IEEE Trans Neural Netw 18(2):416–430

Chen YP, Yu P (2006) Double-Hopf bifurcation in an oscillator with external forcing and time-delayed feedback control. Int J Bifurcation Chaos 16(12):3523–3537

Cooke KL, Grossman Z (1982) Discrete delay, distributed delay and stability switches. J Math Anal Appl 86(2):592–627

Cooke KL, van den Driessche P (1996) Analysis of an SEIRS epidemic model with two delays. J Math Biol 35(2):240–260

Dombovari Z, Wilson R, Stepan G (2008) Estimates of the bistable region in metal cutting. Proc R Soc A-Math Phy Eng Sci 464(2100):3255–3271

Engelborghs K, Luzyanina T, Roose D (2002) Numerical bifurcation analysis of delay differential equations using DDE-BIFTOOL. ACM Trans Math Softw 28(1):1–21

Faria T, Magalhaes LT (1995a) Normal forms for retarded functional differential equations with parameters and applications to Hopf bifurcation. J Differ Equ 122(2):181–200

Faria T, Magalhaes LT (1995b) Normal form for retarded functional differential equations and applications to Bogdanov-Takens singularity. J Differ Equ 122(2):201–224

Gu K, Naghnaeian M (2011) Stability crossing set for systems with three delays. IEEE Trans Autom Control 56(1):11–26

Gu K, Niculescu S-I, Chen J (2005) On stability crossing curves for general systems with two delays. J Math Anal Appl 311(1):231–253

Gu K, Niculescu S-I, Chen J (2007) Computing maximum delay deviation allowed to retain stability in systems with two delays. In: Chiasson J, Loiseau JJ (eds) Applications of time delay systems. Lecture notes in control and information sciences, vol 352. Springer, Berlin, p 157

Guckhenheimerm J, Holmes P (1983) Nonlinear oscillations, dynamical systems and bifurcations of vector fields. Springer, Berlin

Guo S, Huang L (2003) Periodic solutions in an inhibitory two-neuron network. J Comput Appl Math 161(1):217–229

Hale JK (1977) Theory of functional differential equations. Springer, New York

Hale JK, Huang W (1993) Global geometry of the stable regions for two delay differential equations. J Math Anal Appl 178(2):344–362

Hilout S, Boutat M, Laadnani I et al (2010) Mathematical modelling of plastic deformation instabilities with two delays. Appl Math Model 34(9):2484–2492

Hu HY, Wang ZH (2002) Dynamics of controlled mechanical systems with delayed feedback. Springer, Heidelberg

Izhikevich EM (1999) Weakly connected quasi-periodic oscillators, FM interactions, and multiplexing in the brain. SIAM J Appl Math 59:2193–2223

Jia B, Gu H, Li Li et al (2012) Dynamics of period-doubling bifurcation to chaos in the spontaneous neural firing patterns. Cogn Neurodyn 6:89–106

Li Y, Jiang W (2011) Global existence of periodic solutions in the linearly coupled Mackey- Glass system. Int J Bifurcation Chaos 21(3):711–724

Li X, Ruan S, Wei J (1999) Stability and bifurcation in delay-differential equations with two delays. J Math Anal Appl 236(2): 254–280

Liao C-W, Lu C-Y (2011) Design of delay-dependent state estimator for discrete-time recurrent neural networks with interval discrete and infinite-distributed time-varying delays. Cogn Neurodyn 5:133–143

Liao X, Guo S, Li C (2007) Stability and bifurcation analysis in tri-neuron model with time delay. Nonlinear Dyn 49(1):319–345

Liebovitch LS, Peluso PR, Norman MD et al (2011) Mathematical model of the dynamics of psychotherapy. Cogn Neurodyn 5:265–275

Llinas RR (1988) The intrinsic electrophysiological properties of mammalian neurons: a new insight into CNS function. Science 242:1654–1664

Mao X, Hu H (2008) Stability and Hopf bifurcation of a delayed network of four neurons with short-cut connection. Int J Bifurcation Chaos 18(10):3053–3072

Marcus CM, Westervelt RM (1989) Stability of analog neural network with delay. Phys Rev A 39(1):347–359

Marichal RL, Piñeiro JD, González EJ et al (2010) Stability of quasi-periodic orbits in recurrent neural networks. Neural Process Lett 31:269–281

Nakaoka S, Saito Y, Takeuchi Y (2006) Stability, delay, and chaotic behavior in a Lotka- Volterra predator-prey system. Math Biosci Eng 3:173–187

Orosz G, Stepan G (2004) Hopf bifurcation calculations in delayed systems with translational symmetry. J Nonlin Sci 14:505–528

Shayer PL, Campbell SA (2000) Stability, bifurcation, and multistability in a system of two coupled neurons with multiple time delays. SIAM J Appl Math 61(2):673–700

Shi B, Zhang F, Xu S (2011) Hopf bifurcation of a mathematical model for growth of tumors with an action of inhibitor and two time delays. Abstract Appl Anal. doi:10.1155/2011/980686

Sipahi R, Delice II (2009) Extraction of 3D stability switching hypersurfaces of a time delay system with multiple fixed delays. Automatica 45(6):1449–1454

Sipahi R, Niculescu S, Abdallah CT et al (2011) Stability and stabilization of systems with time delay. IEEE Control Syst 31(1):38–65

Song Z, Xu J (2009) Bursting near Bautin bifurcation in a neural network with delay coupling. Int J Neural Syst 19(5):359–373

Song Z, Xu J (2012a) Codimension-two bursting analysis in the delayed neural system with external stimulations. Nonlinear Dyn 67(1):309–328

Song Z, Xu J (2012b) Bifurcation and chaos analysis for a delayed two-neural network with a variation slope ratio in the activation function. Int J Bifurcation Chaos 22(5):1250105

Song Z, Xu J (2012c) Stability switches and multistability coexistence in a delay-coupled neural oscillators system. J Theor Biol 313(21): 98–114

Song Y, Han M, Peng Y (2004) Stability and Hopf bifurcations in a competitive Lotka-Volterra system with two delays. Chaos, Solitons Fractals 22(5):1139–1148

Sun W, Wang R, Wang W et al (2010) Analyzing inner and outer synchronization between two coupled discrete-time networks with time delays. Cogn Neurodyn 4:225–231

Wan A, Wei J (2009) Bifurcation analysis of Mackey-Glass electronic circuits model with delayed feedback. Nonlinear Dyn 57(1): 85–96

Wei J, Zhang C (2008) Bifurcation analysis of a class of neural networks with delays. Nonlinear Anal-Real World Appl 9(5):2234–2252

Xu X (2008) Local and global Hopf bifurcation in a two-neuron network with multiple delays. Int J Bifurcation Chaos 18(4): 1015–1028

Xu S (2009) Hopf bifurcation of a free boundary problem modeling tumor growth with two time delays. Chaos, Solitons Fractals 41(5):2491–2494

Xu J, Pei L (2008) The nonresonant double Hopf bifurcation in delayed neural network. Int J Comput Math 85(6):925–935

Xu X, Hu H, Wang H (2006) Stability switches, Hopf bifurcation and chaos of a neuron model with delay-dependent parameters. Phys Lett A 354(1):126–136

Xu J, Chung KW, Chan CL (2007) An efficient method for studying weak resonant double Hopf bifurcation in nonlinear systems with delayed feedbacks. SIAM J Appl Dyn Syst 6(1):29–60

Yan X-P (2006) Hopf bifurcation and stability for a delayed tri-neuron network model. J Comput Appl Math 196(2):579–595

Ye Q, Cui B (2012) Mean square exponential and robust stability of stochastic discrete-time genetic regulatory networks with uncertainties. Cogn Neurodyn. doi:10.1007/s11571-012-9200-6

Yu P, Yuan Y, Xu J (2002) Study of double Hopf bifurcation and chaos for an oscillator with time delayed feedback. Commun Nonlinear Sci Numer Simul 7(1):69–91

Yuan Y, Campbell SA (2004) Stability and synchronization of a ring of identical cells with delayed coupling. J Dyn Differ Equ 16(3):709–744

Yuan S, Li P (2010) Stability and direction of Hopf bifurcations in a pair of identical tri-neuron network loops. Nonlinear Dyn 61(3):569–578

Zatarain M, Bediaga I, Muñoa J et al (2008) Stability of milling processes with continuous spindle speed variation: analysis in the frequency and time domains, and experimental correlation. CIRP Ann Manuf Techn 57(1):379–384